

# Tunneling conductance of a two-dimensional electron gas with Rashba spin-orbit coupling

B. Srisongmuang and P. Pairor\*

*School of Physics, Institute of Science, Suranaree University of Technology, 111 University Ave., Muang District, Nakhon Ratchasima 30000, Thailand*

M. Berciu

*Department of Physics and Astronomy, University of British Columbia, 6224 Agricultural Road, Vancouver, British Columbia V6T 1Z1, Canada*

(Received 29 May 2008; revised manuscript received 30 July 2008; published 22 October 2008)

We theoretically studied the in-plane tunneling spectroscopy of the hybrid structure composed of a metal and a two-dimensional electron gas with Rashba spin-orbit coupling. We found that the energy spacing between two distinct features in the conductance spectrum can be used to directly measure the Rashba energy. We also considered the effect that varying the probability of spin-conserving and spin-flip scattering at the interface has on the overall conductance. Surprisingly, an increase in interface scattering probability can actually result in increased conductance under certain conditions. Particularly, in the tunneling regime, an increase in spin-flip scattering probability enhances the conductance. It is also found that the interfacial scattering greatly affects the spin polarization of the conductance in metal, but hardly affects that in the Rashba system.

DOI: 10.1103/PhysRevB.78.155317

PACS number(s): 73.40.Ns, 73.40.Gk, 73.23.-b, 72.25.Dc

## I. INTRODUCTION

Structural inversion asymmetry of the confining electrostatic potential results in an intrinsic spin-orbit coupling of electrons in a two-dimensional (2D) electron gas (EG), which can be described by the Rashba Hamiltonian:<sup>1-3</sup>

$$\mathcal{H} = \frac{\vec{p}^2}{2m^*} - \lambda \hat{j} \cdot (\vec{p} \times \vec{\sigma}), \quad (1)$$

where  $\vec{p}$  is 2D momentum,  $m^*$  is the electron effective mass,  $\hat{j}$  is the direction perpendicular to the plane of motion,  $\lambda$  is the spin-orbit coupling parameter, which can be tuned by applying an external gate voltage perpendicular to the 2D plane, and the components of  $\vec{\sigma}$  are the Pauli spin matrices. The spin-orbit interaction lifts the spin degeneracy and causes the original parabolic energy spectrum to split into two branches:  $E_{k,\pm} = \frac{\hbar^2 k^2}{2m^*} \pm \hbar \lambda k$ , where  $k$  is the magnitude of the wave vector. The density of states of this system is the same as that of the 2D free-electron gas for all energies higher than the crossing point of the two branches. However, at the bottom of the band, the density of states has  $E^{-1/2}$  Van Hove singularity because the minus branch has an annular minimum for  $k=k_0 \equiv m^* \lambda / \hbar$  instead of a single-point minimum as in the free-electron gas. These properties lead to interesting phenomena, like the spin Hall effect (see, e.g., Ref. 4 for a review), and to applications in spintronics (see, e.g., Ref. 5 for a review).

The Rashba effect has been seen in many systems such as semiconductors, semiconductor heterostructures, and surface alloys. Several techniques have been used to study the spin-split states in these systems, for example, electron spin resonance, the Shubnikov-de Haas oscillations, angle-resolved photoemission, and scanning tunneling spectroscopy. Electron spin resonance was one of the first techniques to confirm the existence of the Rashba spin-split states in bulk semiconductors with the absence of inversion symmetry in the crystal structure.<sup>6,7</sup> From magnetotransmission of far-infrared radia-

tion, electron spin resonance signal can be detected and used to obtain the Rashba parameter.

The Shubnikov-de Haas oscillations<sup>8,9</sup> is another technique used to measure the Rashba parameter in semiconductor systems. The presence of the spin splitting at the Fermi energy leads to beating in the oscillations and the Rashba energy can be deduced from the position of the beating node. However, this technique tends to provide an overestimate of the Rashba energy, because it is done in the presence of magnetic field and hence includes the effect of the Zeeman spin splitting.<sup>10</sup>

Angle-resolved photoemission spectroscopy and scanning tunneling microscopy are used in surface alloys. The former technique is utilized mainly to obtain the energy dispersion and the Fermi surface map, from which the effective mass, the magnitude of the band splitting, and hence the Rashba spin-orbit coupling energy,  $E_\lambda \equiv \hbar^2 k_0^2 / (2m^*)$ , can be extracted.<sup>11-15</sup> In the latter technique, the electric current is driven through a sharp tip perpendicular to the 2D plane and the differential conductance ( $dI/dV$ ) spectrum can be obtained. One can deduce the Rashba energy by fitting the  $dI/dV$  spectrum to the local density of states of the two-dimensional electron gas (2DEG).<sup>16</sup> In both cases, to obtain information about the Rashba spin-orbit coupling, extensive data fitting is needed.

In this paper, we propose a way to measure the spin-splitting energy more directly from experimental data, using in-plane tunneling spectroscopy. In this technique, the Rashba energy equals the energy difference between two features in the conductance spectrum. The required condition for the measurement is that the energy resolution of the tunneling spectra is at least of the order of the Rashba energy itself. This condition can be easily achieved in modern tunneling measurements.<sup>17</sup>

An intriguing property of 2DEG with Rashba spin-orbit interaction is spin-dependent transport. Many theoretical investigations have shown that both electric and spin transport in hybrid structures between the Rashba system (RS) and

various materials, such as metals,<sup>18–20</sup> ferromagnets,<sup>20–23</sup> and superconductors,<sup>24</sup> are affected by the strength of the spin-orbit coupling,<sup>18–24</sup> the inequality of the effective masses,<sup>18,19,22,23</sup> and the transparency of the interface.<sup>21,22,24</sup> However, in these previous studies, only spin-conserving interfacial scattering was considered.

In principle, one can introduce interfacial spin-flip scattering in these systems by embedding magnetic impurities in the insulating layer, or at the interface. The interaction between the tunneling electrons and localized spins can give rise to spin-flip tunneling.<sup>25–29</sup> The equations describing the spin-up and spin-down spin states in the presence of spin-flip scattering are coupled, and one expects interesting consequences of this. For instance, in the study of the tunneling conductance spectrum of a semiconductor or superconductor junction,<sup>30</sup> the non-spin-flip scattering, when present alone, is found to suppress the Andreev reflection process and hence the subgap conductance as expected. However, when the spin-flip potential scattering is also present at the interface, their combined effect surprisingly enhances the subgap conductance.<sup>30</sup>

Here, we also consider how the scattering potential barrier affects both the conductance spectrum and the spin polarization of the conductance of a junction consisting of a metal and a Rashba system. As in previous work by Zutic and Das Sarma,<sup>30</sup> we find that the conductance spectrum, which is usually suppressed in the presence of the interfacial scattering, can be enhanced by the combined effect of both types of scattering. We also find that the spin polarizations of conductance of the metal and the Rashba system are not equal. The spin polarization in the latter depends weakly on interfacial scattering, while that in the former is greatly affected. This suggests that a spin imbalance in the Rashba system is robust against variation in the quality of the junction interface.

This paper is organized as follows. In Sec. II, we describe the theoretical method and assumptions. In Sec. III, we provide the results and discussion. Our conclusions are presented in Sec. IV.

## II. METHOD OF CALCULATION AND ASSUMPTIONS

We represent our junction by an infinite 2D system which lies on  $xz$  plane, where the metal and the Rashba system occupy the  $x < 0$  and  $x > 0$  region, respectively. The two regions are separated by a flat interface at  $x = 0$ . The interfacial scattering is modeled by a Dirac delta-function potential.<sup>31</sup> We consider ballistic transport in our junction. In the one-band effective-mass approximation, we describe our system by the following Hamiltonian:

$$\mathcal{H} = \left( \hat{p} \frac{1}{2m(x)} \hat{p} + V(x, z) \right) \mathcal{I} + \mathcal{H}_R(x). \quad (2)$$

Each term is the  $2 \times 2$  matrix acting on spinor states,  $\hat{p} = -i\hbar(\hat{x} \frac{\partial}{\partial x} + \hat{z} \frac{\partial}{\partial z})$ . The effective mass  $m(x)$  is position dependent; i. e.,  $[m(x)]^{-1} = m^{-1}\Theta(-x) + (m^*)^{-1}\Theta(x)$ , where  $m$  and  $m^*$  are effective electron masses in the metal and the Rashba system, respectively, and  $\Theta(x)$  is the Heaviside step function.  $V(x, z)$  is also a position-dependent function and is modeled by the expression

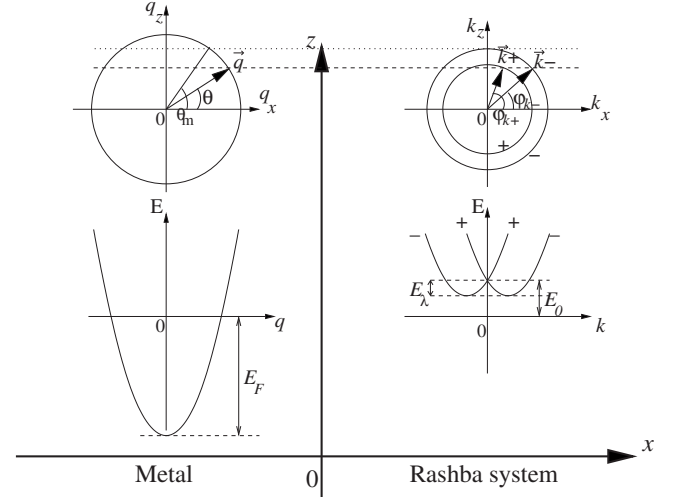


FIG. 1. The top sketches are the energy contours of the electron in the metal (left) and the Rashba system (right). The angles  $\theta$  and  $\varphi$  are defined as those between the  $x$  axis and the momenta of electrons in the metal and the Rashba system, respectively. The dashed line that crosses both sides shows the momentum states with the same  $k_z$ . The dotted line is the line of the maximum value of  $k_z$ , which defines the maximum incident angle  $\theta_m$ . The lower sketches are the corresponding energy spectra ( $E$  vs the magnitude of momentum).  $E_F$  and  $E_0$  are the metal Fermi energy and the off-set energy of the Rashba system, respectively.

$$V(x, z) = H\delta(x) + E_0\Theta(x) - E_F\Theta(-x), \quad (3)$$

where  $H$  represents the scattering potential at the interface,  $E_0$  is the energy difference between the Fermi level and the bottom of the plus branch (see Fig. 1), and  $E_F = \hbar^2 q_F^2 / (2m)$  is the Fermi energy of the metal. We assume that  $E_F$  is much larger than  $E_0$ . The diagonal elements of  $H$ ,  $H_{\uparrow\uparrow}$ , and  $H_{\downarrow\downarrow}$  correspond to the non-spin-flip scattering potential characterizing the quality of the junction, while  $H_{\uparrow\downarrow} = H_{\downarrow\uparrow}$  describe spin-flip scattering.<sup>30</sup> The Rashba Hamiltonian is written as<sup>32</sup>

$$\mathcal{H}_R(x) = \frac{\hat{j}}{2} \cdot [\lambda(x)(\vec{p} \times \vec{\sigma}) + (\vec{p} \times \vec{\sigma})\lambda(x)], \quad (4)$$

where  $\lambda(x) = \lambda\Theta(x)$ .

From the Hamiltonian, one can obtain the eigenstates and eigenenergy for the electrons in each region as follows. In the  $x < 0$  region, the energy spectrum is

$$E(q) = \frac{\hbar^2 q^2}{2m} - E_F, \quad (5)$$

where  $q = \sqrt{q_x^2 + q_z^2}$  is the magnitude of the 2D momentum of the electrons. In the  $x > 0$  region, the eigenenergy is obtained as

$$E^\pm(k) = \frac{\hbar^2}{2m^*} [(k \pm k_0)^2 - k_0^2] + E_0, \quad (6)$$

where  $k = \sqrt{k_x^2 + k_z^2}$  is the magnitude of the 2D momentum and  $k_0 = m^*\lambda/\hbar$ . Figure 1 shows the energy spectra and energy contours of the excitations in both sides of the junction.

The wave function of the electrons with energy  $E$  in the metal is written as a linear combination of incident momentum state and a reflected state of the same energy and  $k_z$ . Because electron spins are not polarized in metal, there are two equally likely incident spin states, opposite in direction to each other, with the spin quantization axis arbitrary. Any choice of two incident states with opposite spin orientations will lead to the same result for total conductance spectrum. Here, for simplicity we choose the spins of the incident electrons be along the  $z$  axis. The two corresponding electron wave functions in the metal are written as

$$\begin{aligned}\Psi_M^{(1)}(x, z) &= \begin{pmatrix} 1 \\ 0 \end{pmatrix} e^{iq_x x} + \begin{pmatrix} b_{1\uparrow} \\ b_{1\downarrow} \end{pmatrix} e^{-iq_x x} e^{ik_z z}, \\ \Psi_M^{(2)}(x, z) &= \begin{pmatrix} 0 \\ 1 \end{pmatrix} e^{iq_x x} + \begin{pmatrix} b_{2\uparrow} \\ b_{2\downarrow} \end{pmatrix} e^{-iq_x x} e^{ik_z z},\end{aligned}\quad (7)$$

where the  $b_{i\sigma}$  are the amplitudes of reflection of electrons with spin  $\sigma$  for incident state with spin up ( $i=1$ ) and spin down ( $i=2$ ).  $q_x = q \cos \theta$  and  $k_z = q \sin \theta$ , where  $\theta$  is the angle between  $\vec{q}$  and the  $x$  axis. The magnitude of the momentum,  $q$ , depends on energy as

$$q = \sqrt{\frac{2m}{\hbar^2}(E + E_F)}. \quad (8)$$

Similarly, in the Rashba system, the wave function is obtained as a linear combination of two outgoing eigenstates of the same energy and  $k_z$ :

$$\begin{aligned}\Psi_{RS}^{(i)}(x, z) &= \begin{pmatrix} c_{i+} \\ \pm \sin \frac{\varphi_{k^+}}{2} \end{pmatrix} e^{\mp ik_x^+ x} \\ &+ c_{i-} \begin{pmatrix} \sin \frac{\varphi_{k^-}}{2} \\ \cos \frac{\varphi_{k^-}}{2} \end{pmatrix} e^{ik_x^- x} e^{ik_z z},\end{aligned}\quad (9)$$

where  $i=1, 2$  refer to the wave functions of the Rashba system corresponding to the two cases of spin orientations of incident electrons,  $\varphi_{k^\pm}$  are the angles between  $\vec{k}^\pm$  and the  $x$  axis. For  $E > E_0$ ,  $c_{i+}$  and  $c_{i-}$  are the transmission amplitudes of electrons to plus and minus branches, respectively. When  $E < E_0$ ,  $c_{i+}$  and  $c_{i-}$  refer to the transmission amplitudes of electrons to states with smaller and larger  $k$  of the minus branch, respectively. The upper and lower signs in the first term of Eq. (9) are for  $E \leq E_0$  and  $E > E_0$ , respectively.  $k_x^\pm = k^\pm \cos \varphi_{k^\pm}$  and  $k_z = k^\pm \sin \varphi_{k^\pm}$ , where the magnitudes of the momenta,  $k^\pm$ , depend on energy as

$$k^- = k_0 + \sqrt{k_0^2 + \frac{2m^*}{\hbar^2}(E - E_0)}, \quad (10)$$

$$k^+ = \pm \left( k_0 - \sqrt{k_0^2 + \frac{2m^*}{\hbar^2}(E - E_0)} \right). \quad (11)$$

Again, in Eq. (11) the upper and lower signs are for  $E \leq E_0$  and  $E > E_0$ , respectively. The relationship between the angles  $\varphi_{k^\pm}$  and  $\theta$  is

$$k^\pm \sin \varphi_{k^\pm} = q \sin \theta. \quad (12)$$

We can obtain the probability amplitudes  $b_{i\uparrow}$ ,  $b_{i\downarrow}$ ,  $c_{i+}$ , and  $c_{i-}$  from the following matching conditions that ensure probability conservation:<sup>32</sup>

$$\Psi_M^{(i)}(x=0, z) = \Psi_{RS}^{(i)}(x=0, z) \equiv \Psi_0^{(i)}, \quad (13)$$

$$\left( \frac{m}{m^*} \frac{\partial \Psi_{RS}^{(i)}}{\partial x} - \frac{\partial \Psi_M^{(i)}}{\partial x} \right) \Big|_{x=0} = \left( 2q_F Z - i \frac{m}{m^*} k_0 \sigma_z \right) \Psi_0^{(i)}, \quad (14)$$

where  $Z = mH/(\hbar^2 q_F)$ . The diagonal elements of  $Z$  will henceforth be referred to as  $Z_u \equiv Z_{\uparrow\uparrow}$  and  $Z_d \equiv Z_{\downarrow\downarrow}$ , while the off-diagonal element will be denoted by  $Z_F = Z_{\uparrow\downarrow} = Z_{\downarrow\uparrow}$ . In what follows the spin-flip term  $Z_F$  will be responsible for the enhancement of a feature at the branch-crossing point in the conductance spectrum.

The particle current density along the  $x$  direction is obtained from

$$j_x^p = \frac{1}{2} \{ \Psi^\dagger(x) \hat{v}_x \Psi(x) + [\hat{v}_x \Psi(x)]^\dagger \Psi(x) \}, \quad (15)$$

where  $\Psi(x)$  is the spinor wave function, and  $\hat{v}_x = d\hat{x}/dt = i[\mathcal{H}(x), \hat{x}]/\hbar$ . From the current density, the reflection and transmission probabilities can be obtained as follows:

$$R_{i\uparrow} = |b_{i\uparrow}|^2, \quad (16)$$

$$R_{i\downarrow} = |b_{i\downarrow}|^2, \quad (17)$$

$$T_{i+} = \frac{m}{m^*} |c_{i+}|^2 \left( \frac{\mp k_x^+ + k_0 \cos \varphi_{k_x^+}}{q_x} \right), \quad (18)$$

$$T_{i-} = \frac{m}{m^*} |c_{i-}|^2 \left( \frac{k_x^- - k_0 \cos \varphi_{k_x^-}}{q_x} \right), \quad (19)$$

where  $R_{i\uparrow}$  and  $R_{i\downarrow}$  are the reflection probabilities to spin-up and spin-down states and  $T_{i+}$  and  $T_{i-}$  are the corresponding transmission probabilities. Also, the upper and lower signs in  $T_{i+}$  are for  $E \leq E_0$  and  $E > E_0$ , respectively. As mentioned earlier, the matching conditions ensure that  $R_{i\uparrow} + R_{i\downarrow} + T_{i+} + T_{i-} = 1$ .

Since the electric current is independent of  $x$ , we consider the electric current density in the metal for simplicity. It can be written as a function of applied voltage  $V$  as follows:

$$\begin{aligned}j_x^e(eV) &= \sum_{q_x > 0, q_z}^2 e v_x \sum_{i=1}^2 (1 - R_{i\uparrow} - R_{i\downarrow}) \\ &\times \{ f[E(q) - eV] - f[E(q)] \},\end{aligned}\quad (20)$$

where  $e$  is the electron charge,  $v_x$  is the  $x$  component of the electron group velocity, and  $f(E)$  is Fermi distribution func-

tion. The sum over the spins of incident electron assumes that both are equally probable in metal.

By changing the integration variable and setting temperature to zero for simplicity, one can obtain the expression for the electric current as

$$j_x^e(eV) = \frac{e \mathcal{L}^2 q_F}{h 2\pi} \int_0^{eV} dE \int_{-\theta_m}^{\theta_m} d\theta \cos \theta \times \sqrt{1 + \frac{E}{E_F} \sum_{i=1}^2 (1 - R_{i\uparrow} - R_{i\downarrow})}, \quad (21)$$

where  $\mathcal{L}^2$  is the area of the metal and  $\theta_m$  is the maximum angle of the incident electrons from the metal (see Fig. 1):  $\theta_m = \sin^{-1}[k^-(E)/q(E)]$ . Thus, the differential conductance  $G(V) \equiv dj_x^e/dV$  at zero temperature is

$$G(V) = \frac{e^2 \mathcal{L}^2 q_F}{h 2\pi} \int_{-\theta_m}^{\theta_m} d\theta \cos \theta \sqrt{1 + \frac{eV}{E_F} \sum_{i=1}^2 (1 - R_{i\uparrow} - R_{i\downarrow})}. \quad (22)$$

The finite temperature will smear the features in the conductance spectrum but will not change their positions (assuming that the strength of the Rashba spin-orbit coupling does not depend on temperature).

It is of interest to determine the spin current across the junction and its dependence on model parameters. However, the appropriate definition of the spin current in a Rashba system is still a matter of debate.<sup>33–37</sup> Here we calculate a simpler, intuitive quantity, which we call the spin polarization of conductance. Our aim is to illustrate the main features of spin-dependent tunneling conductance without entering the controversy over the spin current. The spin polarization of the conductance  $\mathcal{P}(E)$  is defined as the difference in the number of spin carriers crossing a plane normal to  $x$  in unit time, normalized to the total particle current at energy  $E$ ,

$$\mathcal{P}(E) = \frac{\sum_{q_x > 0, q_z} (j_{x,\uparrow}^p - j_{x,\downarrow}^p)}{\sum_{q_x > 0, q_z} (j_{x,\uparrow}^p + j_{x,\downarrow}^p)}, \quad (23)$$

where  $j_{x,\sigma}^p$  is the particle current density with spin  $\sigma$ . The  $\Sigma'$  indicates that the summations are over  $q_x, q_z$  with a specific value of energy  $E$ . In metal, this spin polarization of the conductance can be written in terms of the reflection probabilities as

$$\mathcal{P}_M(E) = \frac{\int_{-\theta_m}^{\theta_m} d\theta \cos \theta \sum_{i=1}^2 (-R_{i\uparrow} + R_{i\downarrow})}{\int_{-\theta_m}^{\theta_m} d\theta \cos \theta \sum_{i=1}^2 (1 - R_{i\uparrow} - R_{i\downarrow})}, \quad (24)$$

and in the Rashba system it can be written in terms of the transmission probabilities as

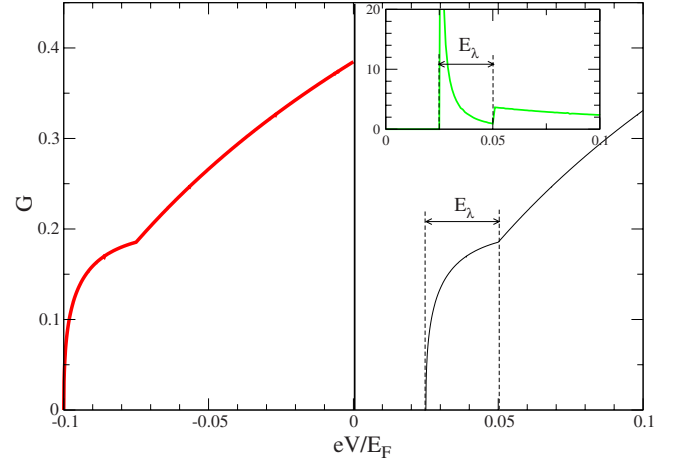


FIG. 2. (Color online) The plot on the left is the conductance spectrum in the case where the energy band of the Rashba system is partly occupied ( $E_0 = -0.075E_F$ ) and on the right is the plot in the case where the band is unoccupied ( $E_0 = 0.05E_F$ ). The derivative of the conductance spectrum on the right ( $dG/dV$ ) is shown in the inset.  $Z$  and  $Z_F$  are set equal to zero.  $m/m^* = 10$  and  $k_0 = 0.05q_F$ .

$$\mathcal{P}_{RS}(E) = \frac{\int_{-\theta_m}^{\theta_m} d\theta \cos \theta \sum_{i=1}^2 (T_{i+} \cos \varphi_{k^+} - T_{i-} \cos \varphi_{k^-})}{\int_{-\theta_m}^{\theta_m} d\theta \cos \theta \sum_{i=1}^2 (T_{i+} + T_{i-})}. \quad (25)$$

As can be seen,  $\mathcal{P}(E)$  measures the relative difference in the net number of the carriers with spin up and spin down. It should be pointed out that in metal  $\mathcal{P}(E)$  is proportional to the conventional spin ( $S_z$ ) current in the  $+x$  direction,  $j_x^s = \text{Re}\{\psi^\dagger \frac{1}{2}(v_x S_z + S_z v_x) \psi\}$ .

### III. RESULTS AND DISCUSSION

In this section, we discuss the effect of the interfacial scattering on the differential conductance spectra and the spin polarization of the conductance on each side of the junction. In all plots, for the purpose of illustration, we set  $m/m^* = 10$  and  $k_0 = 0.05q_F$ , which corresponds to typical experimental values in metal or Rashba system junctions. The main results are not affected by the choice of these parameters.

Two conductance plots for two values of  $E_0$  are shown in Fig. 2. Positive values of  $E_0$  means the energy spectrum of the Rashba system is unoccupied and the positive  $eV$  across the junction will cause the current to flow from the metal to the Rashba system. As can be seen, when the energy spectrum of the Rashba system is partly occupied ( $E_0 = -0.075E_F$ ), the results are identical in shape to those in the unoccupied case ( $E_0 = +0.05E_F$ ), but the applied voltage  $eV$  across the junction has to be negative. There are two main features at the voltage corresponding to the bottom and the branch crossing of the energy band. The distance between them depends on  $E_\lambda$ , which is the quantity of interest. The

value of  $E_0$  is not important; i.e., changing  $E_0$  causes a rigid shift in energy, and will henceforth be set equal to zero.

We do not consider the spin-filtering interface. That is, we set the non-spin-flip scattering strength  $Z_u=Z_d=Z$ . It is well known that the difference in  $Z_u$  and  $Z_d$  will cause a spin-filtering effect. That is, a higher  $Z_u$  will make the transport of the spin-up electrons less favorable and vice versa. This effect cannot be seen in the conductance spectrum and will not be considered in this paper.

### A. Differential conductance spectra

In all conductance plots, the conductance is in units of  $e^2\mathcal{L}^2q_F/(2\pi h)$ . The conductance spectra  $G$  with different  $Z_F$  in different limits of  $Z$  are shown in Fig. 3. Junctions with metallic contacts are characterized by  $Z \ll 1$ , whereas those in the tunneling limit are characterized by  $Z \geq 1$ . In general, the conductance is zero until the applied voltage reaches  $eV = -E_\lambda$ , which is the bottom of the band of the Rashba system. The conductance increases suddenly with large initial slope that decreases steadily until a second feature: the kink occurring at  $eV=0$ , which is the crossing point of the two branches of the band. After this point, the conductance increases approximately linearly. In the presence of  $Z_F$ , there occurs a discontinuity in the conductance at  $eV=0$ . The height of the jump depends on both  $Z$  and  $Z_F$ . *This energy difference between the onset and the discontinuity in the slope of the conductance spectrum can be used to determine directly the Rashba energy  $E_\lambda$ .* Note that this conclusion is not an artifact of this simple model (delta-function interface scattering, etc.). It should be generically true, because it is due to switching from transmission of electrons into only the  $-$  branch to transmission of electrons into both branches of the Rashba system.

In addition to the influence on the discontinuity at  $eV=0$ , the interfacial scattering affects the overall conductance spectrum as well. For metallic contacts, the spin-flip scattering suppresses the conductance as expected. However, in the intermediate and the tunneling limits, the results are rather surprising. As can be seen in Fig. 3(b) when  $Z=0.5$ , the increase in  $Z_F$  from zero to a small value (less than 0.5) does not affect the conductance much. Only when  $Z_F$  is increased beyond 0.5 does the conductance get suppressed. When  $Z$  is high, e.g.,  $Z=2.0$  as in Fig. 3(c), the conductance spectrum can be enhanced by the increase in  $Z_F$  up to a value  $Z_F^*$ , after which the spectrum becomes suppressed.  $Z_F^*$  is found to depend strongly on  $Z$ .

One can see the effect on the conductance spectrum of spin-flip scattering more clearly by considering plots of the conductance  $G$  as a function of  $Z_F$  for energies just below and just above 0. In Fig. 4,  $G^< \equiv G(-\delta)$  and  $G^> \equiv G(+\delta)$ , where  $\delta/E_\lambda=0.8$ , are plotted as a function of  $Z_F$  for different values of  $Z$ . For small  $Z$ , both  $G^>$  and  $G^<$  decrease with  $Z_F$  as expected. However, this trend starts to change when  $Z$  is higher than 0.5. That is, both  $G^>$  and  $G^<$  increase with  $Z_F$  and reach a maximum value at  $Z_F^*$  (as indicated by arrows in Fig. 4), after which they decrease with  $Z_F$ . Notice that  $Z_F^*$  is a little smaller for  $G^<$  than for  $G^>$  and is approximately equal to  $Z$ . It should be noted that a similar dependence of

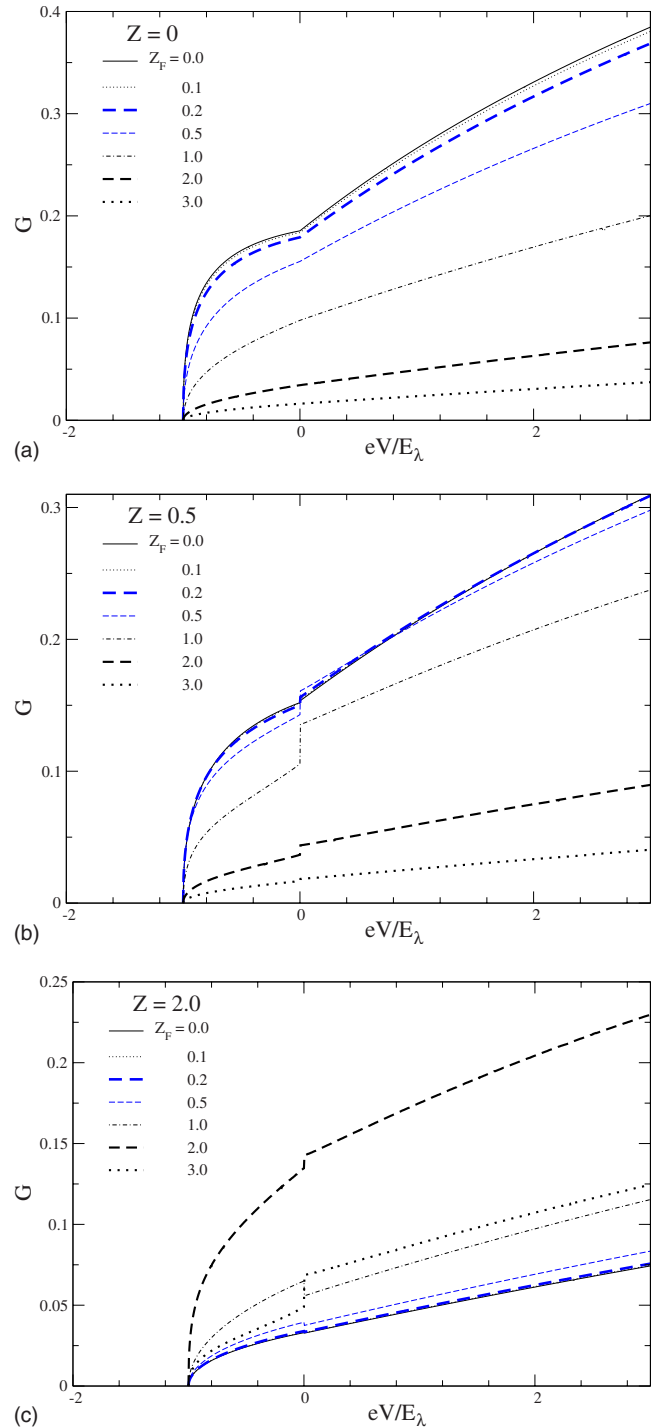


FIG. 3. (Color online) Differential conductance spectra  $G$  for different  $Z_F$  in the case where (a)  $Z=0$ , (b)  $Z=0.5$ , and (c)  $Z=2.0$ .

both  $G^>$  and  $G^<$  on  $Z$  can also be seen, if one plots  $G^>$  and  $G^<$  as a function of  $Z$  instead.

### B. Spin polarization of conductance

The plots of the spin polarizations of the conductance in both metal and Rashba system as a function of energy are shown in Fig. 5. The spin polarizations of the conductance of the two sides are very different. In Rashba system, it is al-

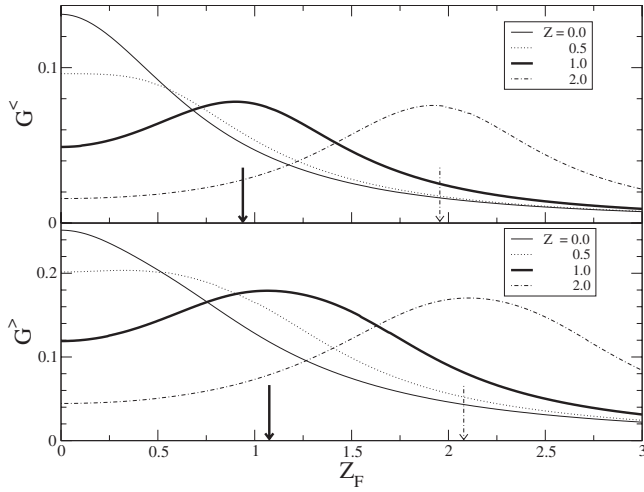


FIG. 4. Differential conductance  $G(eV)$  plotted as a function of the spin-flip barrier height  $Z_F$  at a constant energy  $eV$  slightly below [upper panel, denoted by  $G^<(Z_F)$ ] and slightly above [lower panel, denoted by  $G^>(Z_F)$ ] the energy corresponding to the crossing of the Rashba-split bands. The arrows indicate the values of  $Z_F^*$ , where the maximum differential conductances  $G^>$  and  $G^<$  occur, for  $Z=1.0$  (thick arrows) and  $2.0$  (dashed-dotted arrows).

ways negative, whereas in the metal it is positive when the spin-flip scattering is not strong. This may be understood by considering the density of states of the Rashba system.

The density of states of the minus branch is larger than that of the plus branch. As we can see from Fig. 6, because the spins of the transmitted states of the minus branch are mostly pointing down, it is not surprising that the spin polarization of the conductance in the Rashba system is negative. As for the metal side, because more spin-down states are transmitted into the Rashba system, the spin polarization of the conductance is positive.

The interfacial scattering does not affect the spin polarization of the conductance in the Rashba system as much as in the metal. The increase in either  $Z$  or  $Z_F$  seems to slightly change the magnitude of the spin polarization of the conductance. However, in metal the interfacial scattering potential affects the spin polarization of the conductance a great deal. For a particular value of  $Z$ , the increase in  $Z_F$  can cause the spin polarization of the conductance in metal to change sign.

IV. CONCLUSIONS

According to the results from our simple model, one can directly use in-plane tunneling conductance spectrum to measure the Rashba energy of a system with the Rashba spin-orbit coupling. The energy difference between the onset and the discontinuity in slope of the conductance spectrum is equal to the Rashba energy. Both features are found to be robust against variation in the quality of the junction.

Experimentally, to be able to measure the Rashba energy, the required energy resolution is at least of the order of the Rashba energy itself and the temperature is low enough in order that both features are visible. The Rashba energies in semiconductor-based heterostructures such as InAs, InGaAs,

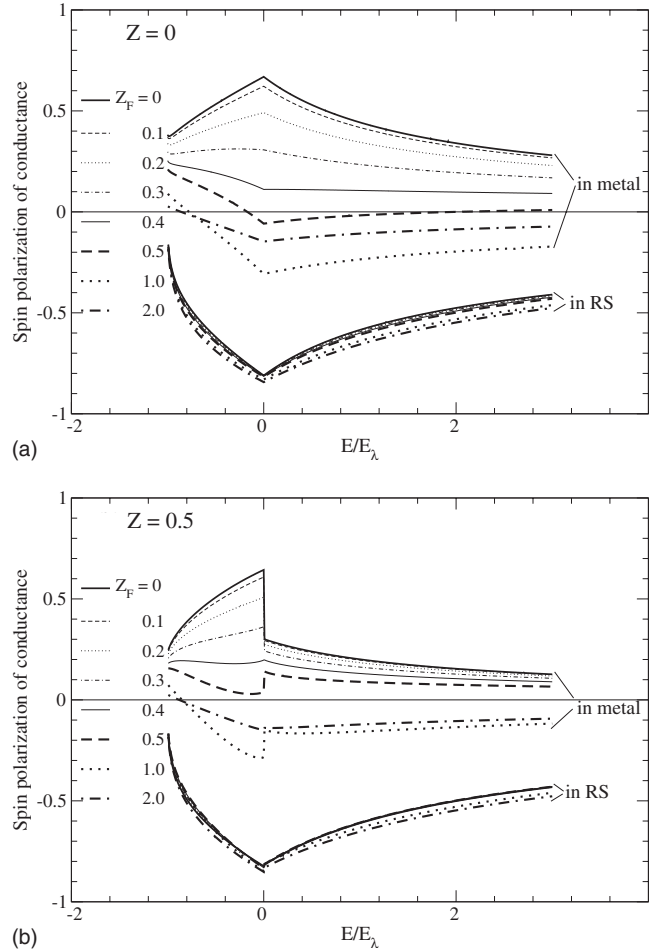


FIG. 5. The plots of the spin polarization of the conductance in metal and RS as a function of energy when  $Z$  is (a) 0 and (b) 0.5.

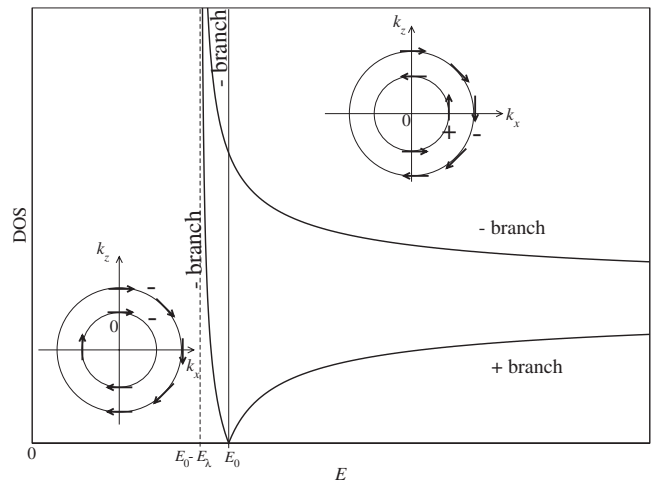


FIG. 6. Density of states of each branch of the 2DEG with the Rashba spin-orbit coupling. The contour plots on the left and on the right are those in the case where  $E < E_0$  and  $E > E_0$ , respectively. When  $E > E_0$ , the outer contour is that of  $-$  branch and the inner one is that of  $+$  branch. When  $E < E_0$ , both energy contours belong to the  $-$  branch. The arrows represent the spin direction of the states with positive  $v_x$ .

GaN, and InSb are of order 1–3 meV,<sup>38–45</sup> whereas those of surface alloys like Li/W(110), Pb/Ag(111), and Bi/Ag(111) can be as large as 200 meV.<sup>16,46–48</sup> These conditions can be readily met in modern tunneling measurements.<sup>17</sup>

We also found that as the current is driven through the system, an imbalance of spin in both sides occurs. The spin polarization of the conductance in the metal is found to depend strongly on both types of the interfacial scattering and can disappear when the barrier is in the tunneling regimes. On the contrary, in the Rashba system the spin polarization of the conductance is always present and only slightly affected by interfacial scattering. This finding suggests that the spin imbalance caused by current flow in the system with the

Rashba spin-orbit coupling is robust against variation in the quality of the junction as well.

#### ACKNOWLEDGMENTS

We thank M. F. Smith for a critical reading of the manuscript. Also, we would like to acknowledge financial support from Thailand Cooperative Research Network (Physics). P.P. thanks Thailand Research Fund and Commission on Higher Education (Grant No. RMU488012 and CHE-RES-RG “Theoretical Physics”) for financial support. M.B. was supported by the Research Corporation, CIFAR, and NSERC.

\*pairor@sut.ac.th

- <sup>1</sup>E. I. Rashba, *Sov. Phys. Solid State* **2**, 1109 (1960).
- <sup>2</sup>Y. A. Bychkov and E. I. Rashba, *J. Phys. C* **17**, 6039 (1984).
- <sup>3</sup>Y. A. Bychkov and E. I. Rashba, *JETP Lett.* **39**, 78 (1984).
- <sup>4</sup>H. Engel, E. I. Rashba, and B. I. Halperin, *Handbook of Magnetism and Advanced Magnetic Materials* (Wiley, Chichester, 2007).
- <sup>5</sup>I. Zutic, J. Fabian, and S. Das Sarma, *Rev. Mod. Phys.* **76**, 323 (2004).
- <sup>6</sup>B. D. McCombe, S. G. Bishop, and R. Kaplan, *Phys. Rev. Lett.* **18**, 748 (1967).
- <sup>7</sup>B. D. McCombe and R. J. Wagner, *Phys. Rev. B* **4**, 1285 (1971).
- <sup>8</sup>J. Nitta, T. Akazaki, H. Takayanagi, and T. Enoki, *Phys. Rev. Lett.* **78**, 1335 (1997).
- <sup>9</sup>G. Engels, J. Lange, Th. Schäpers, and H. Lüth, *Phys. Rev. B* **55**, R1958 (1997).
- <sup>10</sup>G. Lommer, F. Malcher, and U. Rössler, *Phys. Rev. Lett.* **60**, 728 (1988).
- <sup>11</sup>S. LaShell, B. A. McDougall, and E. Jensen, *Phys. Rev. Lett.* **77**, 3419 (1996).
- <sup>12</sup>F. Reinert, *J. Phys.: Condens. Matter* **15**, S693 (2003).
- <sup>13</sup>J. Henk, M. Hoesch, J. Osterwalder, A. Ernst, and P. Bruno, *J. Phys.: Condens. Matter* **16**, 7581 (2004).
- <sup>14</sup>H. Cercellier, Y. Fagot-Revurat, B. Kierren, F. Reinert, D. Popović, and D. Malterre, *Phys. Rev. B* **70**, 193412 (2004).
- <sup>15</sup>D. Popović, F. Reinert, S. Hüfner, V. G. Grigoryan, M. Springborg, H. Cercellier, Y. Fagot-Revurat, B. Kierren, and D. Malterre, *Phys. Rev. B* **72**, 045419 (2005).
- <sup>16</sup>C. R. Ast, G. Wittich, P. Wahl, R. Vogelgesang, D. Pacilé, M. C. Falub, L. Moreschini, M. Papagno, M. Grioni, and K. Kern, *Phys. Rev. B* **75**, 201401(R) (2007).
- <sup>17</sup>E. L. Wolf, *Principles of Tunneling Spectroscopy* (Oxford University Press, New York, 1989).
- <sup>18</sup>G.-H. Liu and G.-H. Zhou, *Chin. Phys. Lett.* **22**, 3159 (2005).
- <sup>19</sup>M. Lee and M. S. Choi, *Phys. Rev. B* **71**, 153306 (2005).
- <sup>20</sup>V. M. Ramaglia, D. Bercioux, V. Cataudella, G. De Filippis, C. A. Perroni, and F. Ventriglia, *Eur. Phys. J. B* **36**, 365 (2003).
- <sup>21</sup>C. M. Hu and T. Matsuyama, *Phys. Rev. Lett.* **87**, 066803 (2001).
- <sup>22</sup>T. Matsuyama, C. M. Hu, D. Grundler, G. Meier, and U. Merkt, *Phys. Rev. B* **65**, 155322 (2002).
- <sup>23</sup>Y. Jiang and M. B. A. Jalil, *J. Phys.: Condens. Matter* **15**, L31 (2003).
- <sup>24</sup>T. Yokoyama, Y. Tanaka, and J. Inoue, *Phys. Rev. B* **74**, 035318 (2006).
- <sup>25</sup>F. Guinea, *Phys. Rev. B* **58**, 9212 (1998).
- <sup>26</sup>P. Lyu, D. Y. Xing, and J. Dong, *Phys. Rev. B* **58**, 54 (1998).
- <sup>27</sup>J. Inoue and S. Maekawa, *J. Magn. Magn. Mater.* **198-199**, 167 (1999).
- <sup>28</sup>R. Jansen and J. S. Moodera, *Phys. Rev. B* **61**, 9047 (2000).
- <sup>29</sup>A. Vedyayev, D. Bagrets, A. Bagrets, and B. Dieny, *Phys. Rev. B* **63**, 064429 (2001).
- <sup>30</sup>I. Zutic and S. Das Sarma, *Phys. Rev. B* **60**, R16322 (1999).
- <sup>31</sup>G. E. Blonder, M. Tinkham, and T. M. Klapwijk, *Phys. Rev. B* **25**, 4515 (1982).
- <sup>32</sup>U. Zülicke and C. Schroll, *Phys. Rev. Lett.* **88**, 029701 (2001).
- <sup>33</sup>E. I. Rashba, *Phys. Rev. B* **68**, 241315(R) (2003).
- <sup>34</sup>Q.-F. Sun and X. C. Xie, *Phys. Rev. B* **72**, 245305 (2005).
- <sup>35</sup>J. Shi, P. Zhang, D. Xiao, and Q. Niu, *Phys. Rev. Lett.* **96**, 076604 (2006).
- <sup>36</sup>E. B. Sonin, *Phys. Rev. B* **76**, 033306 (2007).
- <sup>37</sup>Q.-F. Sun, X. C. Xie, and J. Wang, *Phys. Rev. B* **77**, 035327 (2008).
- <sup>38</sup>S. Sasa, K. Anjiki, T. Yamaguchi, and M. Inoue, *Physica B (Amsterdam)* **272**, 149 (1999).
- <sup>39</sup>D. Grundler, *Phys. Rev. Lett.* **84**, 6074 (2000).
- <sup>40</sup>T. Matsuyama, R. Kürsten, C. Meissner, and U. Merkt, *Phys. Rev. B* **61**, 15588 (2000).
- <sup>41</sup>T. Koga, J. Nitta, T. Akazaki, and H. Takayanagi, *Phys. Rev. Lett.* **89**, 046801 (2002).
- <sup>42</sup>K. Fujii, Y. Morikami, T. Ohyama, S. Gozu, and S. Yamada, *Physica E (Amsterdam)* **12**, 432 (2002).
- <sup>43</sup>I. Lo, J. K. Tsai, W. J. Yao, P. C. Ho, L. W. Tu, T. C. Chang, S. Elhamri, W. C. Mitchel, K. Y. Hsieh, J. H. Huang, H. L. Huang, and W. C. Tsai, *Phys. Rev. B* **65**, 161306(R) (2002).
- <sup>44</sup>G. A. Khodaparast, R. C. Meyer, X. H. Zhang, T. Kasturiarachchi, R. E. Doezema, S. J. Chung, N. Goel, M. B. Santos, and Y. J. Wang, *Physica E (Amsterdam)* **20**, 386 (2004).
- <sup>45</sup>G. A. Khodaparast, R. E. Doezema, S. J. Chung, K. J. Goldammer, and M. B. Santos, *Phys. Rev. B* **70**, 155322 (2004).
- <sup>46</sup>E. Rotenberg, J. W. Chung, and S. D. Kevan, *Phys. Rev. Lett.* **82**, 4066 (1999).
- <sup>47</sup>D. Pacilé, C. R. Ast, M. Papagno, C. Da Silva, L. Moreschini, M. Falub, A. P. Seitsonen, and M. Grioni, *Phys. Rev. B* **73**, 245429 (2006).
- <sup>48</sup>C. R. Ast, J. Henk, A. Ernst, L. Moreschini, M. C. Falub, D. Pacilé, P. Bruno, K. Kern, and M. Grioni, *Phys. Rev. Lett.* **98**, 186807 (2007).